3.2.Results and Discussion

3.2.1 F^+ Laser oscillation and related properties

3.2.1.1 F^+ laser oscillation

The configuration coordinate data of F^+ centers at the low coordinated surfaces of CaO are given in Table 2 and the configuration coordinate curves are given in Fig.3. The strength of the electron- phonon coupling as reflected by the shifts in the equilibrium positions $Q_3 - Q_1$ and the values of Stokes shifts between the ground states and excited states suggests that F^+ laser oscillation fades quickly as the oxygen coordination decreases from 5(flat) to 4 (edge) to 3 (corner), thus making the flat surface the most attractive compared with the edge and corner sites.

The strong dependence of the absorption and emission energies, and consequently Stokes-shifts, on ion coordination is probably due to the combination of several factors. Some of these factors have already been discussed by Garrone, Zecchina, and Stone [56] and include the reduction of the Madelung potential at low coordinated sites, which leads to their substantial relaxation with respect to ideal geometry and to strong electron-density redistribution. However, the reduction of the Madelung potential alone cannot quantitatively explain the experimental data. This is perhaps not surprising because, as is demonstrated in the calculations of Shluger et al. [62], both the degree of localization of the excited state and its nature depend on its location. Strong localization of the excited states on certain sites makes the Madelung argument less applicable.

With small Stokes shift, the optical-optical conversion efficiency will be increased. On the other hand, the reabsorption of emitted light by other F^+ centers will also be increased. If the negative effect of reabsorption is stronger than the positive effect due to the conversion efficiency, then the

laser activity will be decreased. Inspection of Table 2, reveals that the negative effect of reabsorption is dependent on surface coordination. In other words, the negative effect of reabsorption increases when one goes from the flat(5) to the edge(4) to the corner(3) surface.

A laser suitable defect should have relaxed excited states deep below the conduction band of the perfect crystal [54]. To examine this issue, we consider the band structure of CaO surface i.e the positions of the one lectron defect levels with respect to the perfect surface bands. In Table 3, we present the tops of the valence bands VB and the bottoms of the conduction bands CB for the ground states of the defect free surfaces as well as the highest occupied molecular orbitals HOMOs and the lowest unoccupied molecular orbitals LUMOs for the relaxed excited states of the defect containing surfaces. As shown all relaxed excited states defect levels LUMOs are below the lower edges of the conduction bands of the defect free surfaces CB by ca. 2.36-2.46 eV implying that F^+ is a laser suitable defect. Based on stokes-shifed optical transition bands, the CaO surface provides F^+ laser oscillation significantly stronger than that of SrO.

3.2.1.2 RES orientational destruction

One consequence of the relaxed excited state RES saddle point configuration of F^+ center is a temperature independent ionic reorientation during the pump cycle, i.e. a change of the center axis into a perpendicular (equivalent) orientation. This effect can be understood from Fig. 4 where it is seen that after the emission process the bulk or surface anion has a chance of hopping to the <110> anion vacancy site opposite to its starting location. Therefore, if an F^+ center system is excited in either one of its absorption bands with polarized light having

its propagation direction parallel to a <100> axis and the electric field vector **E** parallel to a perpendicular <100> axis, the F^+ centers excited by the **E**-vector will quickly switch to <100> directions where they are no longer excited and the system will become experimentally transparent for the excitation light [54].

To examine the RES orientational destruction of F^+ theoretically, we calculated the total electronic energies of the original RES ion configuration (Δ=0.0) and the RES ion configurations obtained by moving one of the next nearest neighbor anions to the defect site along the <110> axis (Δ=0.25, 0.50, 0.75 and 1). In each case the nearest neighbor cations to the defect site were relaxed to equilibrium. The total electronic energies of the RES ion configurations as function of the migration path Δ are given in Fig 5. The differences between the energies of the original RES ion configuration and the RES saddle point ion configuration (the energy barriers to orientational destruction in laser experiment) are given in Table 4. As shown in Table 4 and Fig.5, the orientational destruction of F^+ center depends on the location of the anionic species as well as the surface coordination number. The destruction of F^+ by surface oxygen was easier than that by bulk oxygen,and while the flat surface was relatively the most probable surface for orientational destruction of F^+ by bulk oxygen, the corner surface was relatively the most probable surface for orientational destruction of F^+ by surface oxygen. Since the energy barrier to the migration of surface oxygen at the corner surface is smaller than the energy barrier to the migration of bulk oxygen at the flat surface, we may conclude that the least laser active corner is fortunately the most probable site for orientational destruction of F^+. Experimentally, in order to avoid orientational destruction, the pump polarization and direction of

propagation of the pump beam inside the crystal have to be chosen such that they are not parallel to a <100> direction. While the barrier hights of the RES orientational destruction of F^+ center at the low coordinated surfaces of CaO due to the migration of the surface anions were significantly smaller than those of SrO, the barrier hights due to the migration of the bulk anions were significantly greater than these of SrO.

3.2.1.3. Reorientation efficiency and optical memories

It is possible to use the reorientation properties of defects under the action of polarized light to store information [55]. The reorientation efficiency is directly proportional to the recording sensitivity. Since the reorientation efficiency of the present F^+ center depends on surface coordination number, we may expect from Table 4, a relatively high recording sensitivity for the flat surface due to the migration of bulk oxygen, and for the corner surface due to the migration of surface oxygen. Since the energy barrier to the migration of surface oxygen at the corner surface is smaller than the energy barrier to the migration of bulk oxygen at the flat surface, we may expect the corner surface to give the maximum possible recording sensitivity. While the recording sensitivity of CaO due to the migration of the surface O^{2-} is greater than that of SrO, the recording sensitivity of CaO due to the migration of bulk O^{2-} is significantly smaller than that of SrO.

3.2.1.4 Exciton (energy) transfer

Excitation transfer for vibronic materials was first formulated by Forster and Dexter [63]. Orbach [64] discussed the factors affecting excitation transfer between ions in vibronic laser materials, gave examples of the important excitation transfer mechanisms and introduced

a new method for utilization of collision induced electric dipole radiation and collision induced excitation transfer in the solid state.

The relative total energies of the excited states at different low coordinated surface sites could be used as the first indicator of whether the exciton excited at a particular surface site would transfer to another site. In order to be able to compare the results for different shapes and sizes of quantum clusters, the relative energies of the excited states for different coordinations were estimated following the method of Shluger, et al. [30]. The ionization energies I for the clusters were calculated using the CIS method. Assuming the vacuum level for all systems considered, the ground state total energies were placed at –I as shown in Fig.6. Then the energies of the excited states were located with respect to the defined positions of the ground states using the excitation energies. As can be seen from Fig.6, the excited state at the edge site has the highest energy relative to the flat and corner sites. The excited state at the edge has higher energy than that at the flat surface, and the latter is higher than at the corner. In other words the relative energies at the low coordinated surfaces of CaO are sensitive to F^+ imperfection and there is a possibility for exciton transfer from the edge site to the other coordinated flat and corner sites. Cox and Williams [65] argued that the excited state at the surface is in the positive spectrum. Shluger, et al.[30] suggested that it could has negative values for MgO. Our estimates suggest that it could has only positive values for CaO, in agreement with the estimates of Cox and Williams. The exciton energy transfer of CaO is generally greater than that of SrO.

3.2.1.5 F^+ relaxation and formation energies

Since F^+ laser activity is related to surface coordination, an attempt has been made to calculate F^+ relaxation and formation energies at the low coordinated surfaces of CaO. Surface relaxation energies were calculated subtracting the total electronic energy of the relaxed configuration (relaxed to equilibrium) from that of the unrelaxed configuration

$$\Delta E_{relaxation} = E_{unelaxed} - E_{relaxed} \quad (2)$$

Surface relaxation energies are given in Table 5, from which we conclude that surface relaxation energies decrease with decreasing the surface coordination number. This means that the flat surface requires the largest amount of energy to relax to equilibrium.

Surface defect formation energies or defect creation probability were calculated by subtracting the sum of the total energies of the reactants from those of the products

$$\Delta E_{formation} = \Delta E_{products} - \Delta E_{reactants} \quad (3)$$

Here the reactants are the defect free surfaces, and the products are the F^+ defect containing surfaces (relaxed to equilibrium) and O^- anions. The defect formation energies are given in Table 6, from which we conclude that F^+ defect formation energies decrease with decreasing the surface coordination number. This means that the most laser active flat surface requires the largest amount of energy to create the F^+ center. In other words, the F^+ center at the most laser active flat surface, enjoys the largest continued stability although it needs the largest amount of energy to relax to equilibrium.

With a few exception, the relaxation and defect formation energies of F^+ at the reduced oxygen coordination of CaO are equivalent to these of SrO.

3.2.1.7 The Glasner -Tompkins relation

Glasner and Tompkins [66] reported an empirical relationship between the principal optical absorption of F centers in solids and the fundamental absorption of the host crystal. The difference between the first exciton absorption energy E_X and the F band energy E_F was found to depend almost exclusively on the negative ion species. In other words, the Glasner-Tompkins empirical rule suggests that the energy difference between the fundamental absorption of an alkali halide and the F band is very nearly a function of the halide species alone. E_X, E_F, E_X-E_F and $<E_X$-$E_F>$ for twelve alkali halides have been reported by Malghani and Smith [67], and for LiH and LiF by Shalabi et al.[68]. The dependence of Glasner-Tompkins relation on the dopant cation and surface coordination number of MgO, KCl and AgBr has also been reported by Shalabi et al.[69]. Here we make an additional attempt to generalize this relation to include the low coordinated surfaces of CaO.

To apply the Glasner-Tompkins relation to the present F^+ center, we have to calculate the corresponding band gaps and exciton bands. A complete treatment to understanding the host dependence of band gaps would involve theories of excitons [70] and defects[71]which take into account the band structure. Since this will be a major undertaking and well beyond our present goal, we will use the simple electron transfer model of the fundamental optical absorption of ionic solids developed by Hilsch and Pohl [72]. This model, in its simplest form, explains the fundamental optical absorption E_X as the transfer of an electron from a negative ion to a neighboring positive ion both placed adjacent to the

defect site. It seems likely that all color centers have perturbed excitons formed near them [73]. We have therefore calculated E_X as the change in Coulomb energy, associated with the transfer of either one or two electrons E_{X1} and E_{X2} from an oxide anion to a neighboring strontium cation, both placed adjacent to the F^+ center, and calculate E_{F^+} as the energy difference between the HOMO and LUMO energy levels. The correlation between the oxide ion coordination, the F^+ center and the energy difference between the exciton bands E_{X1} and E_{X2}, and band gaps E_{F^+} are given in Table 7. As one can see from Table 7, the results emphasize the dependence of the energy differences on the oxide coordination. The energy difference was reduced as the oxide ion coordination decreases generalizing in turn the Glasner-Tompkins relation to include the surface coordination of CaO. The difference between the F^+ band gaps and exciton bands of CaO surfaces are generally greater than those of SrO.

3.2.2 The halogen-surface interactions

3.2.2.1 Electrostatic potentials

To shed light on the possible electrostatic contributions to the halogen – surface interactions of the defect free and defect containing surfaces, we calculated the electrostatic potential curves at the oxygen site of the defect free surface and the F^+ site of the defect containing surface. The electrostatic potential curves are shown in Figure 7, from which we conclude that the electrostatic potentials due to the defect free and defect containing surfaces are very different for adsorbate-substrate interactions, leading thus to different electric fields and electric field derivatives. Since the electrostatic interaction of the adatom with the surface will mainly consist of electric-field induced dipole and electric

field derivatives-induced quadrupole moments, one expects that the classical contributions to the adsorbate-substrate interactions are very different for the defect free and defect containing surfaces of CaO.

3.2.2.2 Adsorbate-substrate interactions

To examine the adsorbate-substrate interactions of the title halogens (F,Cl and Br) under the effect of F^+ imperfection, we calculated the adsorption energies on two equivalent sites, the oxygen ion site of the defect free surface and the F^+ site of the defect containing surface, Figure 8. The nearest and next nearest neighbor ions to the oxygen or F+ site are considered in the calculations. The nearest neighbor ions to the F^+ site were first allowed to relax to equilibrium. The adsorbate-substrate distances were then optimized in each case. The corresponding results of the equilibrium adsorbate-substrate distances and interactions (adsorption energies) are collected in Table 8.

We may first note that the adsorption site over the oxygen atom is the energetically most favorable as confirmed by experimental data [74] and LDA-type calculations [75]. Now, as shown in Table 8, the interaction energies of the considered halogens with the oxygen site of the defect free surface were endothermic, while those with the F^+ site of the defect containing surface were exothermic and the adsorbates were electronically stable. The F^+ center enhances the adsorption energies of halogens significantly and changes the nature of adsorption from physical adsorption to chemical adsorption assuming a boundary value of ca.-1.5 eV between both types of adsorption. The order of adsorption energies on both of the defect free and defect containing surfaces is essentially the same : F>Cl>Br, pointing to a dependence on the periodic properties of group VIIB halogens. While the calculated adsorption energy was directly proportional to the electronegativity of the halogen, the

calculated adsorbate-substrate distance was inversely proportional. The F atom penetrates the surface layer of the defect containing surface and offers the maximum adsorbate-substrate interactions.

The significant increase in adsorption energies due to F^+ may be explained on basis of spin pairing between the halogen single electron and F^+ single electron. Here, the term "covalent spin pairing" may be suggested instead of " spin pairing" since the later is based on the view of rigid two particles, while the former expresses the sense of smearing and overlapping. On the other hand, the pattern of adsorption energies is consistent with that already expected from the electrostatic potential curves, where distinct differences in adsorption energies occur between the defect free and the defect containing surfaces. The adsorption energies of the halogen F, Cl and Br are smaller than these of SrO.

3.2.2.3 The roles of energy gaps and covalent spin pairing

To clarify the roles of (i) the energy gap between the adsorbate and the substrate, and (ii) the spin pairing between the adsorbate single electron and the substrate F^+ electron, in the course of adsorbate-substrate interactions, we calculated the highest occupied atomic orbital HOAO and the lowest unoccupied atomic orbital LUAO for each of the considered halogens, the top of the valence band VB and the bottom of the conduction band CB of the defect free surface, and the highest occupied molecular orbital HOMO and the lowest un occupied molecular orbital LUMO of the defect containing surface. The calculated energy levels are presented in Fig. 9.

As shown in Fig.9, covalent spin pairing is only allowed between the halogen and the defect containing surface. The strength of adsorption follows the order F>Cl>Br despite that the energy gaps between the HOAOs of the halogen atoms and the HOMO of the defect containing

surface increase from Br to Cl to F. This implies that the covalent spin pairing, rather than the energy gap factor, plays the dominant role in the course of adsorbate-substrate interactions, and that the large increase in adsorption energies following surface imperfection is mainly attributed to the role of covalent spin pairing.

3.2.2.4 Band gaps and electrical conductivity

Figure 9 shows that the defect free surface of CaO can not be made semiconducting by F^+ imperfection. The band gap of the defect free surface was not reduced to a value less than 2 eV, which is the domain of band gaps of a semiconducting material. However, the narrowing of band gaps suggests that the electrical conductivity of the insulator CaO can be enhanced under the effect of the F^+ trapped electron in analogy with the behavior of the F trapped electron in alkali hydrides and halides.These is no significant differences in the F^+ enhancement of electrical conductivity between CaO and SrO.

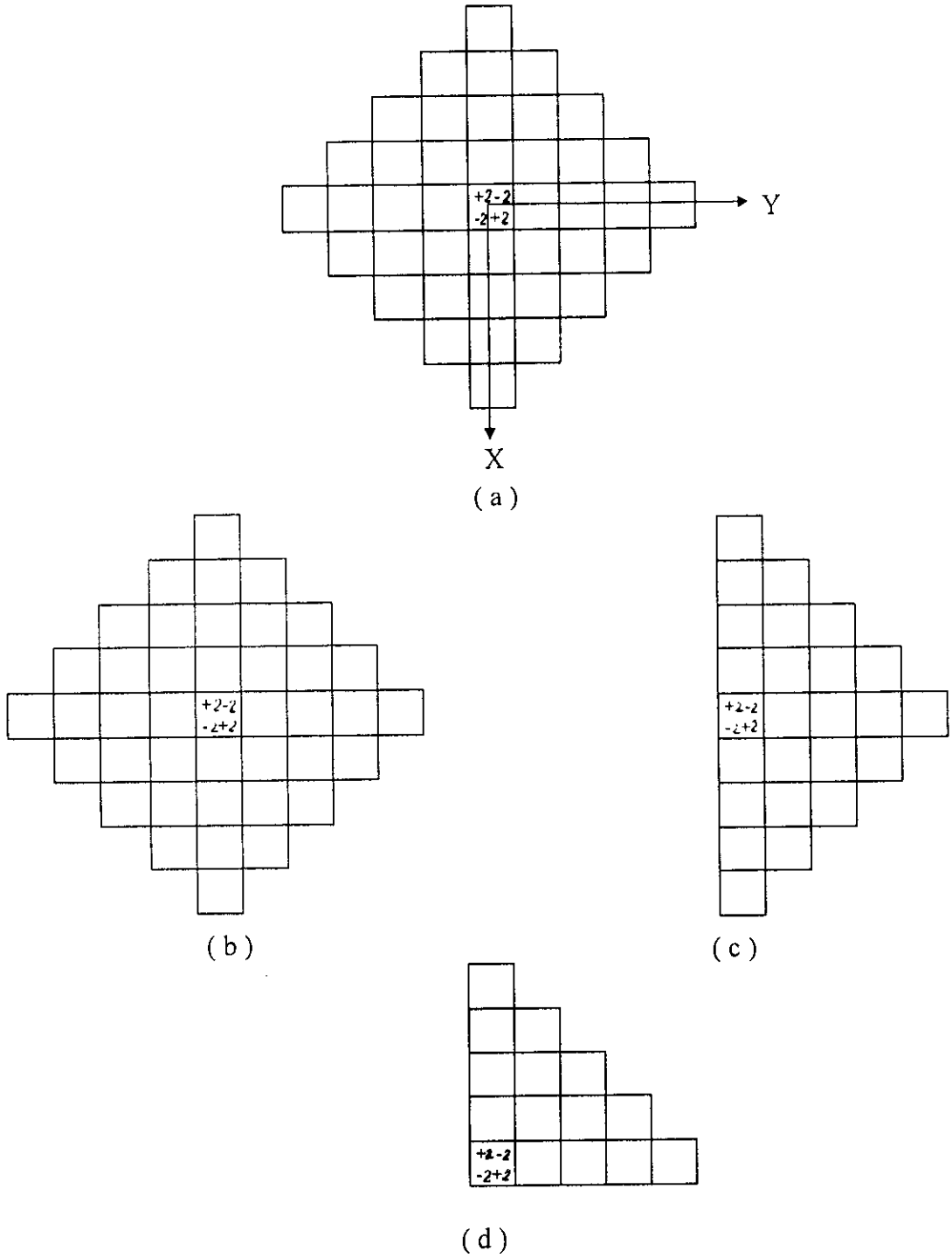

Figure 1: Z = 0 plane representation of the CaO crystal considered in the calculations.
(a) bulk (b) Flat (c) Edge (d) Corner

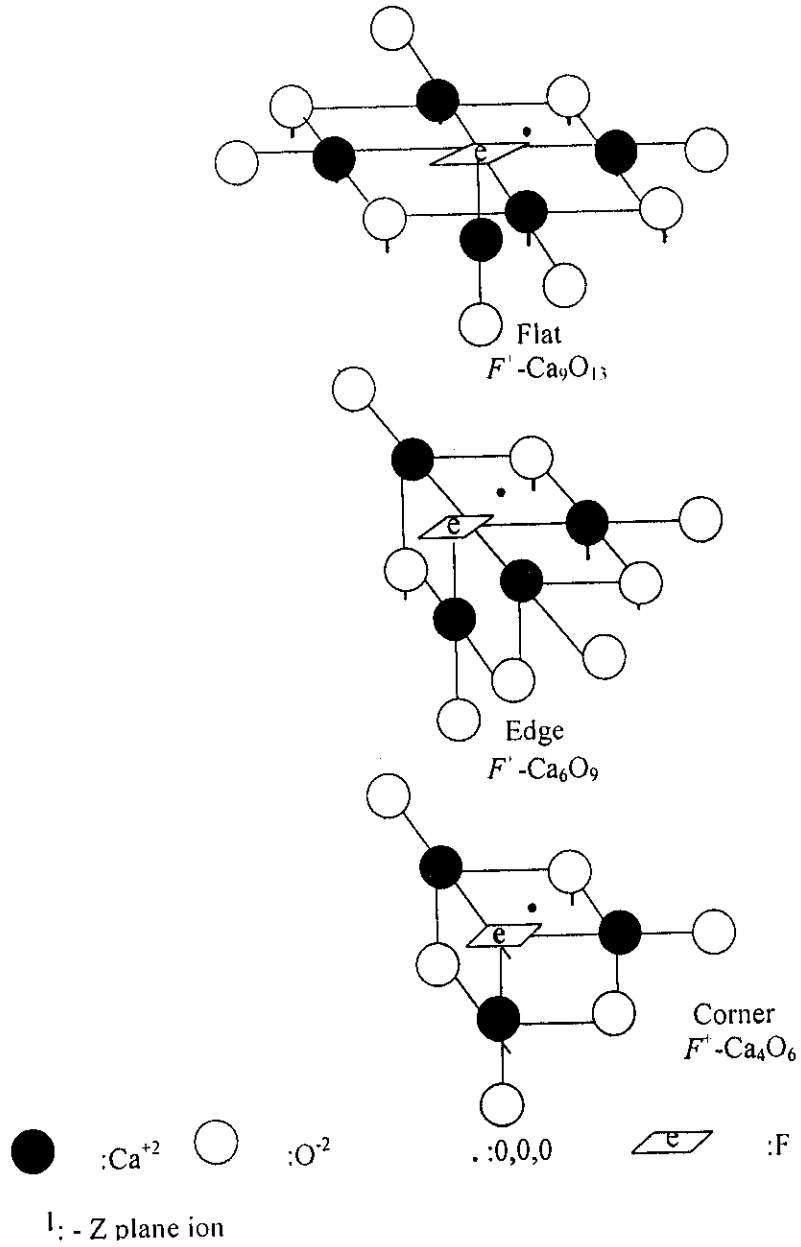

Figure 2: The low coordinated surface clusters considered in the calculations.

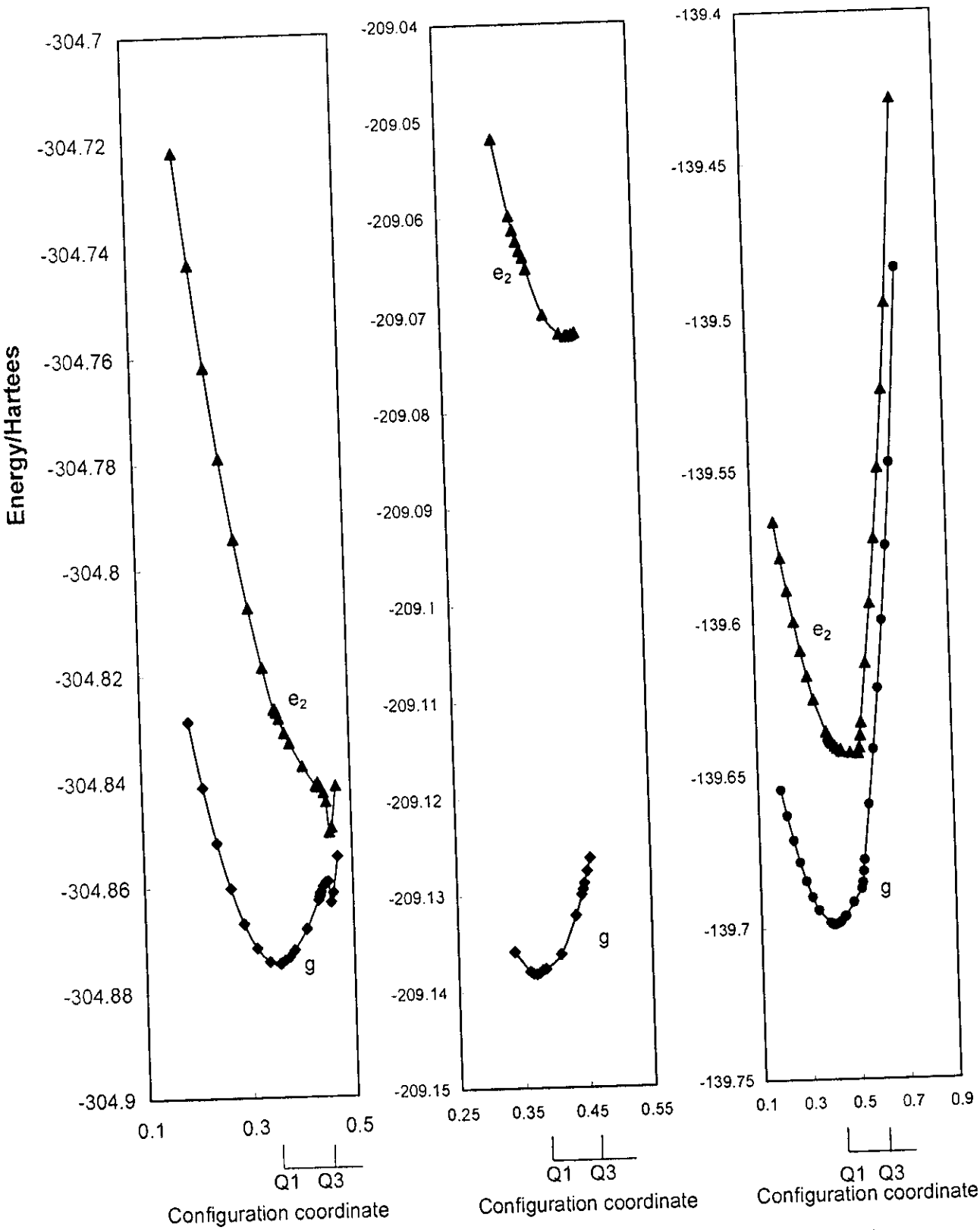

Fig.(3): The configuration coordinate diagarms of the low coordinate surfaces of CaO with F^+ color center. Minima of the ground state (Q_1) and second doublet excited state (Q_3) g: doublet e_2:second doublet excited state.

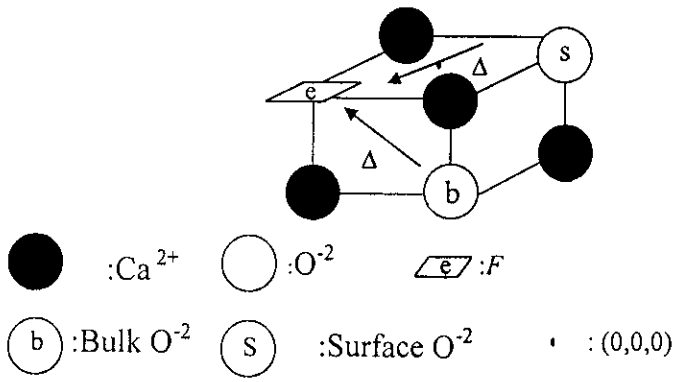

Figure 4: Representation of the RES ion configurations responsible for orientational destruction of F^+ center at the low coordinated surfaces of CaO.

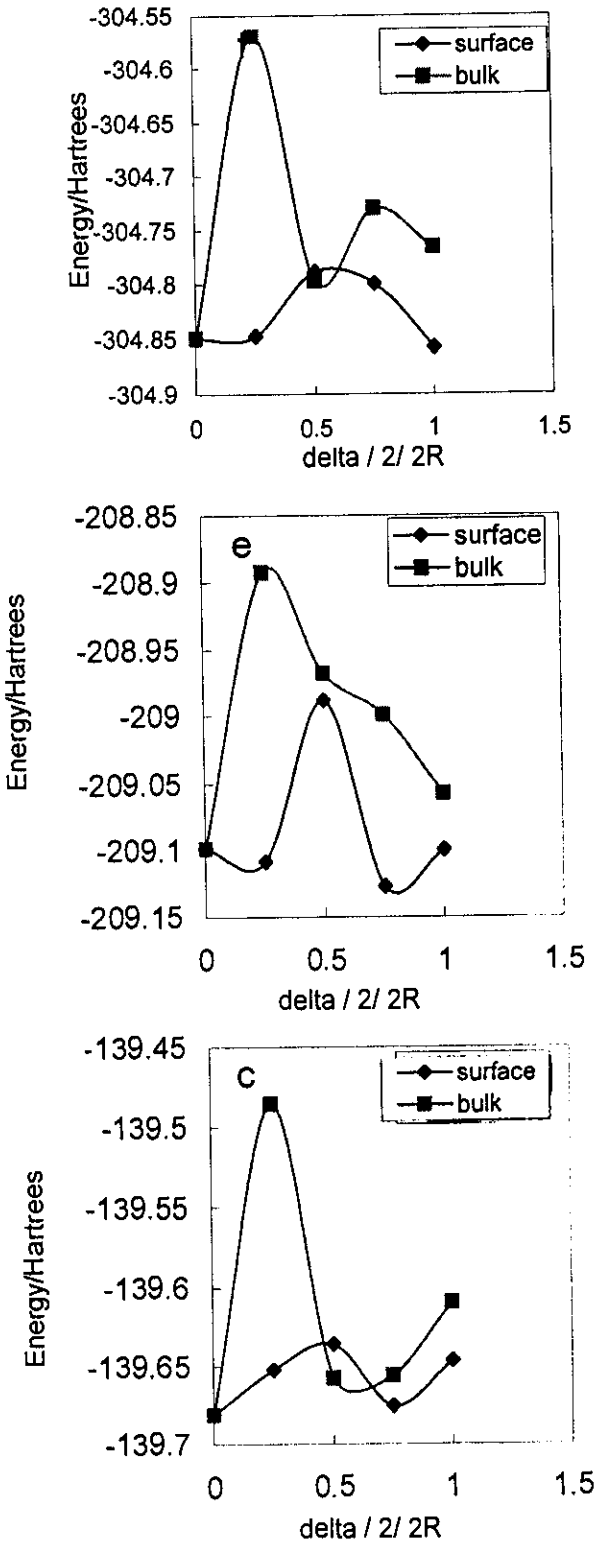

Fig.5: The energetics of the RES orientational destruction of F^+ center at the low coordinated surfaces of CaO due to the migration of the bulk and surface anions along <110> axis f:flat e:edge c:corner

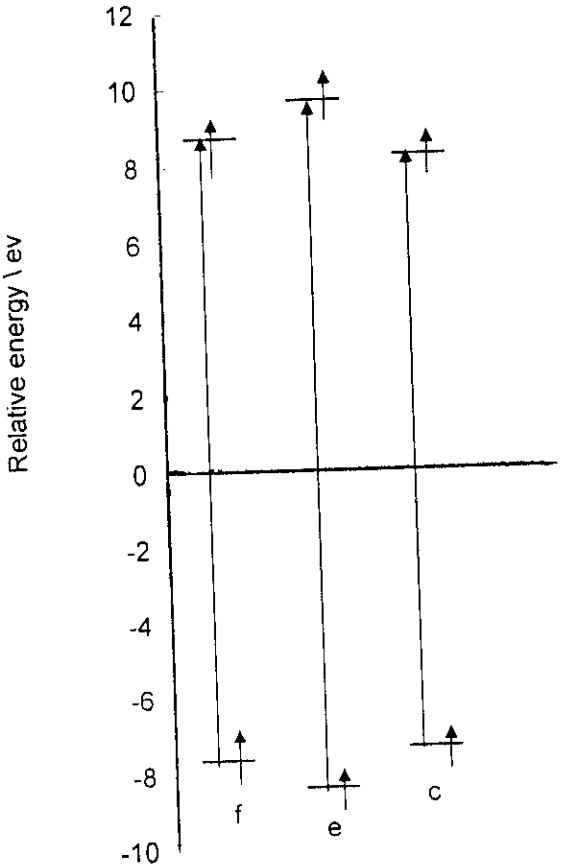

Figure 6:Diagram representing the relative energies of the ground and excited states of the low coordinated surface sites of CaO using the CIS method. f:flat ,e:edge ,c:corner

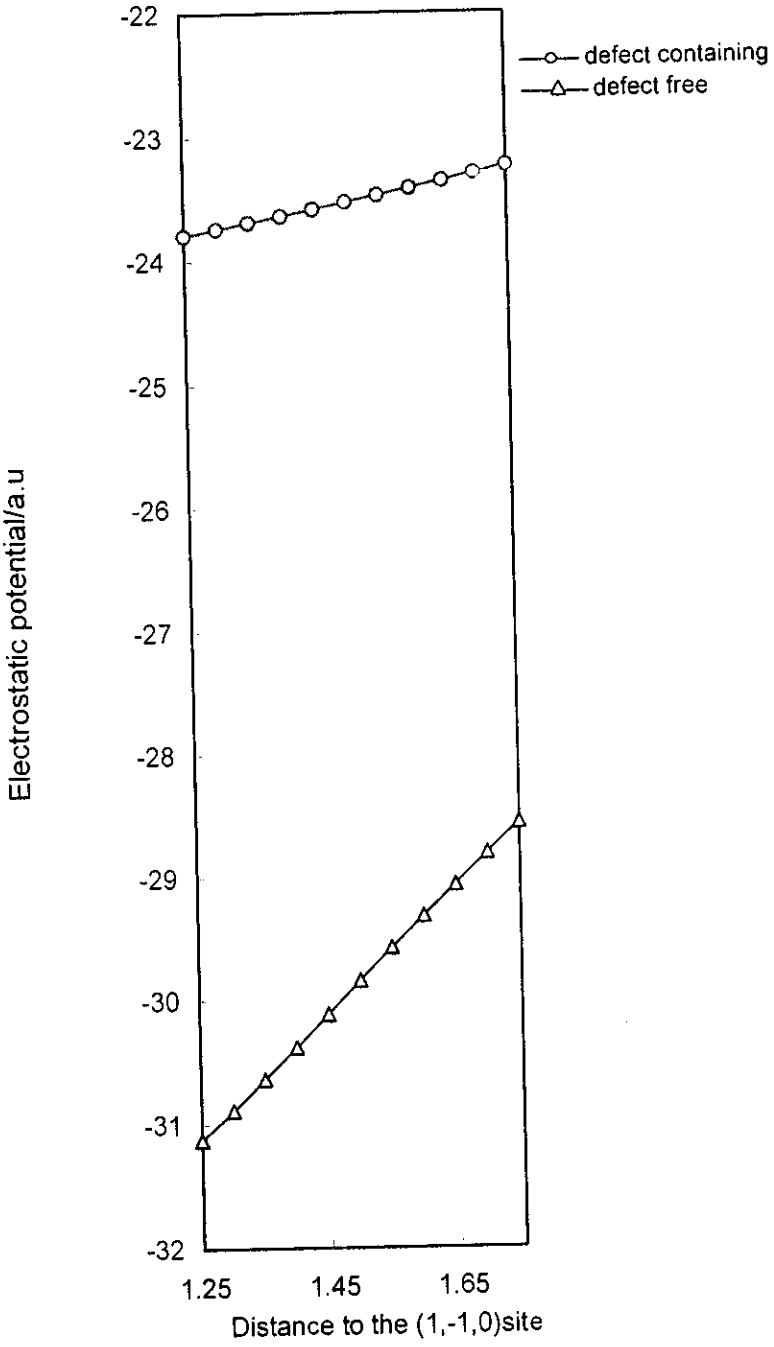

Figure 7: Electrostatic potentials of defect free Ca_9O_{14} and defect-containing F^+ -Ca_9O_{13} surfaces of CaO.

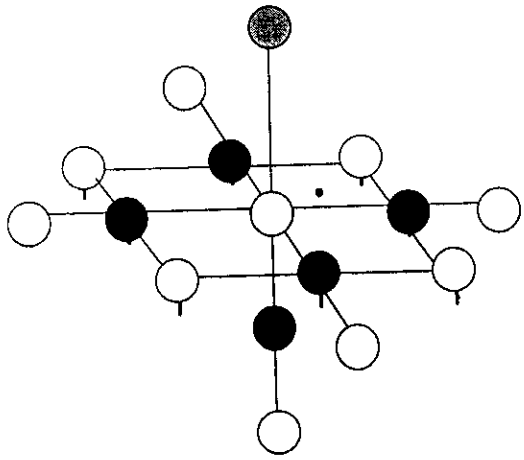

Ca_9O_{14}

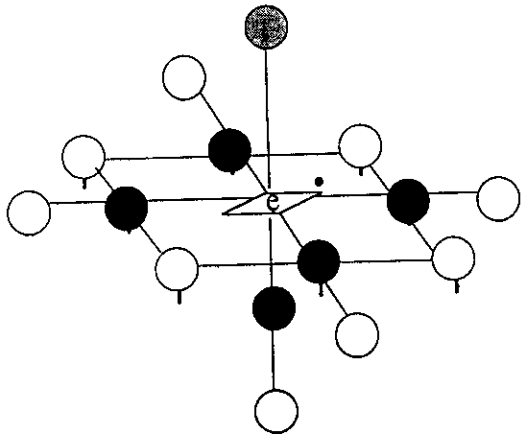

$F^+Ca_9O_{13}$

:Ca^{+2} :O^{-2} :0,0,0 e :F

| : - Z plane ion :F,Cl,Br

Figure 8: The adsorption of F, Cl and Br over the defect free (Ca_9O_{14}) and defect containing (F^+-Ca_9O_{13})surfaces of CaO.

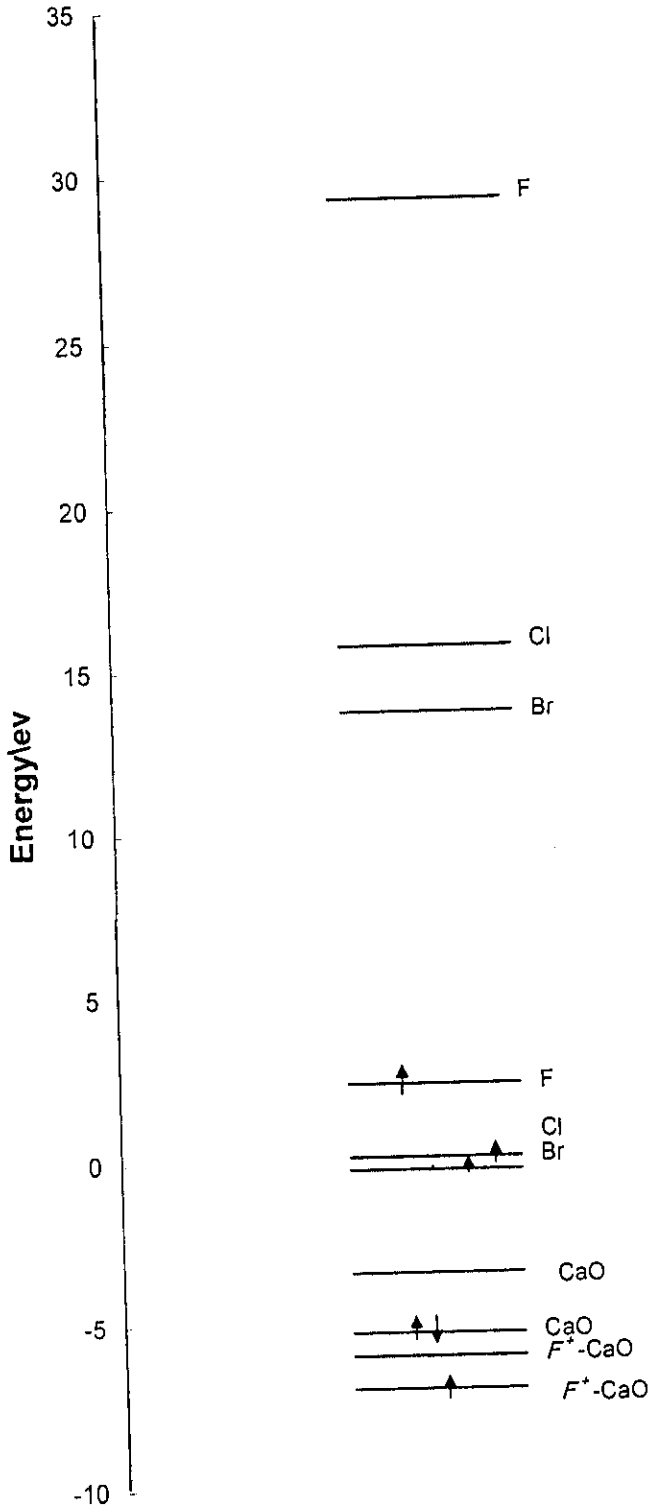

Figure 9: HOMOs and LUMOs of the halogen atoms F,Cl and Br,VB and CB of free surface (Ca_9O_{14}) and HOMO and LUMO of the defect containing surface (F^+-Ca_9O_{13}) .

Table 1: Specification of the finite lattices used for Bulk, Flat, Edge, and corner surfaces of CaO. R is half the lattice distance, which for CaO is 2.11 Å, and r is the distance of the appropriate shell from the center of the lattice.

	Bulk		Flat		Edge		Corner		
r^2/R^2	Coordinates/R (±X), (±Y), (±Z)	Number of centers	Coordinates/R (±X)(±Y)(Z≤0)	Number of centers	Coordinates/R (±X), (Y≥-1) (Z≤0)	Number of centers	Coordinates/R (X≤1), (Y≥-1), (Z≤0)	Number of centers	Charge |q|
2	1 1 0	4	1 1 0	4	1 1 0	4	1 1 0	4	2
6	1 1 2	8	1 1 2	4	1 1 2	4	1 1 2	4	2
10	3 1 0	8	3 1 0	8	3 1 0	6	3 1 0	4	2
14	3 1 2	16	3 1 2	8	3 1 2	6	3 1 2	4	2
18	1 1 4	8	1 1 4	4	1 1 4	4	1 1 4	4	2
18	3 3 0	4	3 3 0	4	3 3 0	2	3 3 0	1	2
22	3 3 2	8	3 3 2	4	3 3 2	2	3 3 2	1	2
26	5 1 0	8	5 1 0	8	5 1 0	6	5 1 0	4	2
26	3 1 4	16	3 1 4	8	3 1 4	6	3 1 4	4	2
30	5 1 2	16	5 1 2	8	5 1 2	6	5 1 2	4	2
34	3 3 4	8	3 3 4	4	3 3 4	2	3 3 4	1	2
34	5 3 0	8	5 3 0	8	5 3 0	4	5 3 0	2	2
38	5 3 2	16	5 3 2	8	5 3 2	4	5 3 2	2	2
38	1 1 6	8	1 1 6	4	1 1 6	4	1 1 6	4	2
42	5 1 4	16	5 1 4	8	5 1 4	6	5 1 4	4	2
46	3 1 6	16	3 1 6	8	3 1 6	6	3 1 6	4	2
50	5 5 0	4	5 5 0	4	5 5 0	2	5 5 0	1	2
50	5 3 4	16	5 3 4	8	5 3 4	4	5 3 4	2	2
50	7 1 0	8	7 1 0	8	7 1 0	6	7 1 0	4	2
54	5 5 2	8	5 5 2	4	5 5 2	2	5 5 2	1	2
54	3 3 6	8	3 3 6	4	3 3 6	2	3 3 6	1	2
58	7 3 0	8	7 3 0	8	7 3 0	4	7 3 0	2	2
66	5 5 4	8	5 5 4	4	5 5 4	2	5 5 4	1	2
54	7 1 2	16	7 1 2	8	7 1 2	6	7 1 2	4	0.818566
62	7 3 2	16	7 3 2	8	7 3 2	4	7 3 2	2	0.818566
66	1 1 8	8	1 1 8	4	1 1 8	4	1 1 8	4	1.601818
82	9 1 0	8	9 1 0	8	9 1 0	6	9 1 0	4	1.601818
86	9 1 2	16	9 1 2	8	9 1 2	6	9 1 2	4	1.601818
		Σ=292		Σ=176		Σ=120		Σ=81	

Table (2) : Minima of the ground state (Q_1), the excited state (Q_3), horizontal shifts along the configuration coordinate (Q_3-Q_1) for absorbed and emission transition energies Δ E between the ground state (g) and the excited state (e_1) of F^+ center at CaO surface calculated at the CIS level. All lengths are given in Å and energies in eV.

	Q_1	Q_3	Q_3-Q_1	$\Delta E_{absorption}$ ($g \rightarrow e_2$)	$\Delta E_{emission}$ ($g \leftarrow e_2$)	Stokes-shifts
Flat	0.356	0.457	0.101	1.301	0.361	0.940
Edge	0.370	0.445	0.075	2.061	1.559	0.502
Corner	0.399	0.481	0.082	1.652	1.343	0.309

Table 3: The tops of valence bands VB and the bottoms of conduction bands CB of the defect free surfaces in the ground states and the HOMOs and LUMOs of the defect containing surfaces in the relaxed excited states of the low coordinated surfaces of CaO. Energies are given in eV.

	Defect free surfaces ground states		**Defect containing surfaces relaxed excited states**	
	VB	**CB**	**HOMO**	**LUMO**
Flat	**-8.77**	**-1.51**	**-6.88**	**-4.09**
Edge	**-7.46**	**-1.72**	**-7.89**	**-4.27**
Corner	**-5.83**	**-0.88**	**-6.87**	**-3.50**

Table 4: The barrier heights of the RES orientational destruction of F^+ center at the low coordinated surfaces of CaO due to the migration of the bulk and surface anions along the <110> axes. Energies are given in Hartrees.

	Bulk O^{-2}	Surface O^{-2}
Flat	0.382	0.092
Edge	0.339	0.095
Corner	0.259	0.059

Table 5: Equilibrium relaxation energies of the defect containing surfaces of CaO calculated at the DFT level. Energies are given in eV.

Flat	**2.75**
Edge	**2.49**
Corner	**1.99**

Table 6: The defect formation energies of CaO surface calculated at the DFT level. Energies are given in eV.

Flat (Ca_9O_{14})	$\longrightarrow$ $F^+ - Ca_9O_{13} + O^-$	**12.570**
Edge (Ca_6O_{10})	$\longrightarrow$ $F^+ - Ca_6O_9 + O^-$	**11.653**
Corner (Ca_4O_7)	$\longrightarrow$ $F^+ - Ca_4O_6 + O^-$	**6.347**

Table 7: F^+ band gaps E_{F^+} and exciton bands E_{x1} and E_{x2} of the defect containing surfaces of CaO calculated at the DFT level. Energies are given in eV.

	E_{F^+}	E_{x1}	E_{x2}	$E_{x1} - E_{F^+}$	$E_{x2} - E_{F^+}$
Flat	1.005	33.56	50.63	32.64	49.62
Edge	1.181	32.89	49.30	31.71	49.12
Corner	1.064	30.57	44.79	29.51	43.73

Table 8: Optimal adsorption energies $E_{ads.}$ and adsorbate –substrate distances R_e of F, Cl and Br over the defect free and defect containing flat surfaces of CaO calculated at the DFT level. Energies are given in eV and distances in Å.

	F		Cl		Br	
	R_e	$E_{ads.}$	R_e	$E_{ads.}$	R_e	$E_{ads.}$
Ca_9O_{14}	2	0.495	2.4	1.654	2.5	1.851
F^+- Ca_9O_{13}	-0.2	-5.760	0.7	-3.04	1.2	-2.04